# $e^+e^- \to p\bar{p}$ @ CMD-3

Ivanov Daniil on behalf of the CMD-3 collaboration

# VEPP-2000 collider


Electron-positron collider

Covers c.m. energy range from 0.36 to 2.0 GeV

Two experiments – CMD-3 and SND

| Design parameters @ 1 GeV | |
|---|---|
| Circumference | 24.388 m |
| Beam energy | 150 ÷ 1000 MeV |
| N of bunches | 1×1 |
| N of particles | $1\times10^{11}$ |
| Betatron tunes | 4.14 / 2.14 |
| Beta* | 8.5 cm |
| BB parameter | 0.1 |
| Luminosity | $1\times10^{32}$ $cm^{-2}s^{-1}$ |

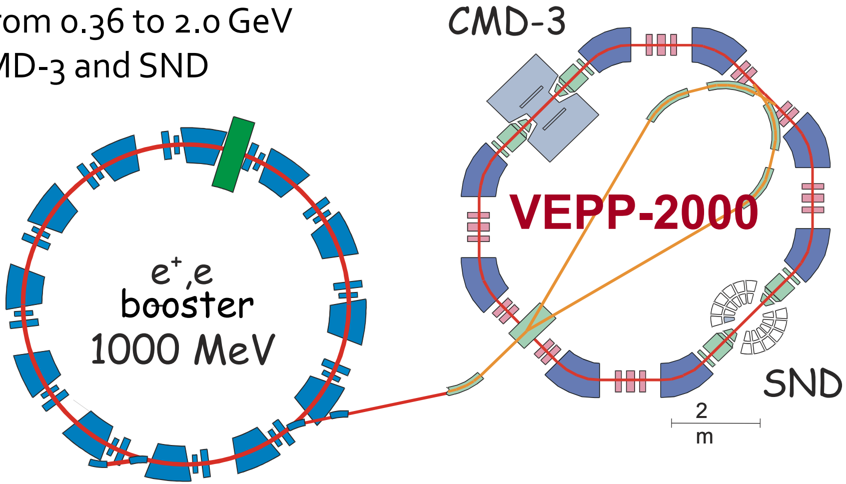


"Round beam" optics

Energy monitoring by Compton backscattering ($\sigma_{\sqrt{s}} \approx 0.1$ MeV)

# VEPP-2000

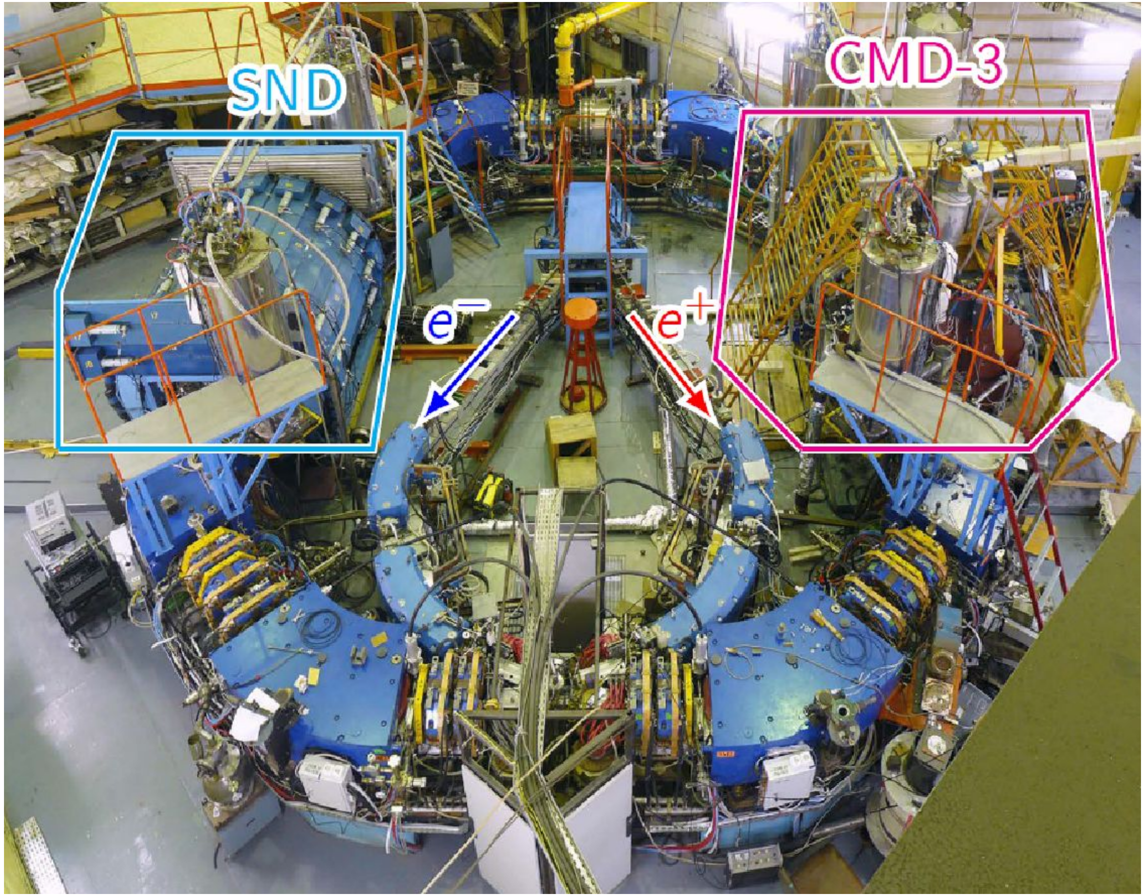

# CMD-3 Detector

*Cryogenic Magnetic Detector

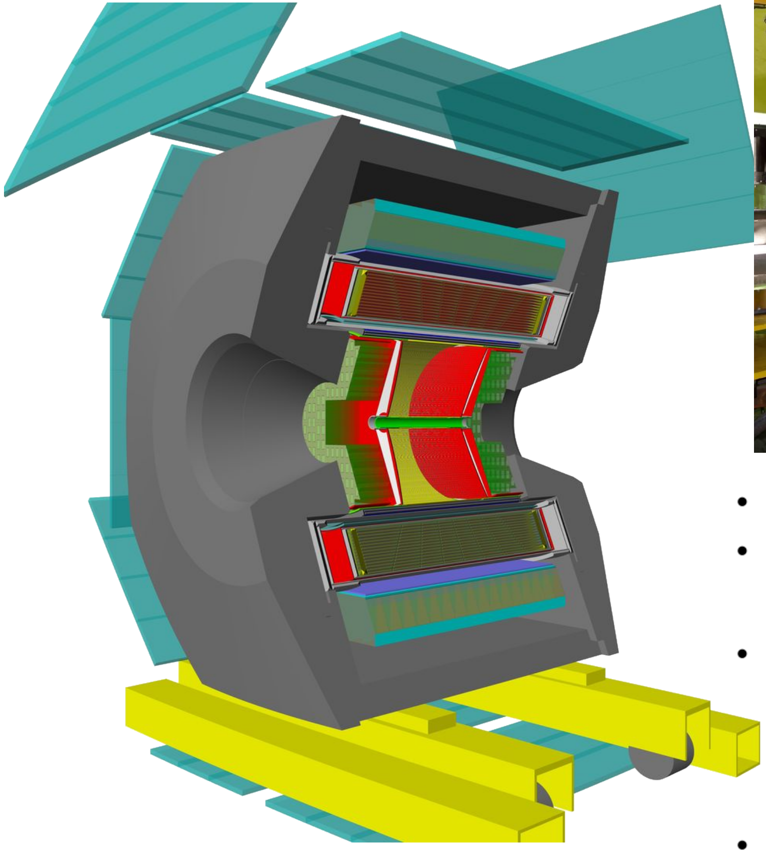

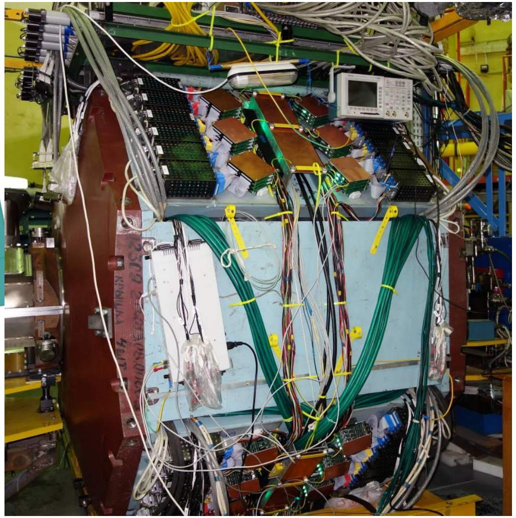

- Magnetic field 1.0-1.3T
- Drift chamber
  - ➢ $\sigma_{R\varphi} \sim 100\ \mu, \sigma_z \sim 2-3$ mm
- EM calorimeter (LXE, CsI, BGO), 13.5 $X_0$
  - ➢ $\sigma_E/E \sim 3\% - 10\%$
  - ➢ $\sigma_\Theta \sim 5$ mrad
- TOF
- Muon counters

$$e^+e^- \to p\bar{p}$$

# Collected data

The initial goal of **∫Ldt = 1 fb$^{-1}$** was achieved this year.

Data collection continues.

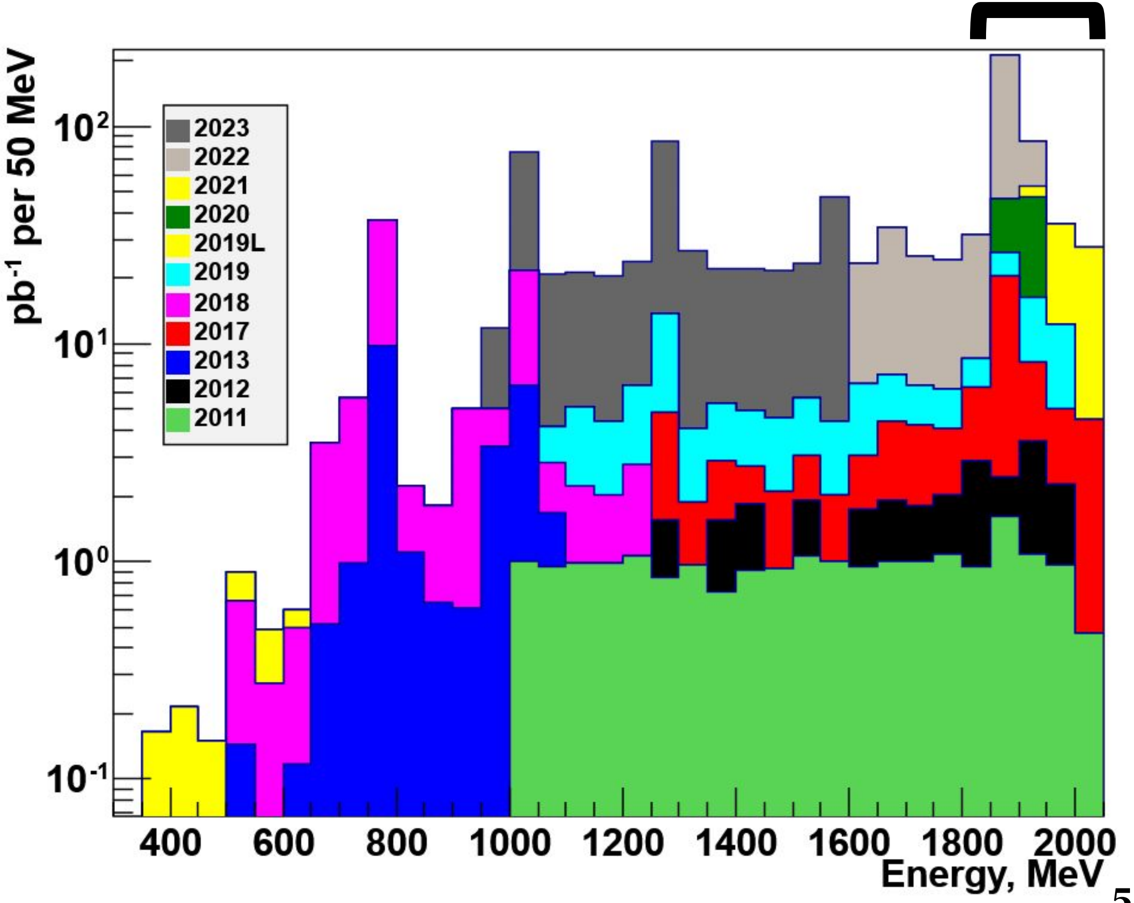

# CMD-3 final states under analysis

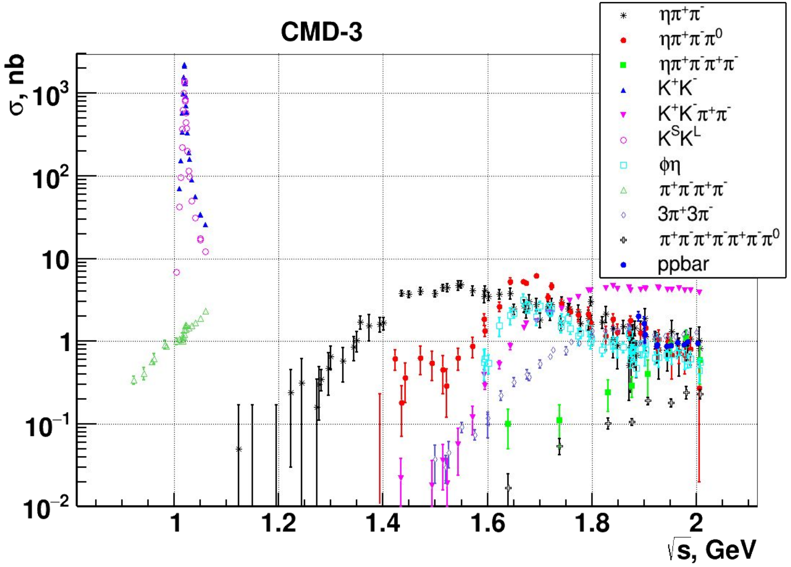


| Signature | Final states (preliminary, published) |
|---|---|
| 2 charged | $\pi^+\pi^-$, $K^+K^-$, $K_SK_L$, $p\bar{p}$ |
| 2 charged + $\gamma$'s | $\pi^+\pi^-\gamma, \pi^+\pi^-\pi^0, \pi^+\pi^-\eta, K^+K^-\pi^0, K^+K^-\eta, K_SK_L\pi^0$, $K_SK_L\eta, \pi^+\pi^-\pi^0\eta, \pi^+\pi^-2\pi^0, \pi^+\pi^-3\pi^0, \pi^+\pi^-4\pi^0$ |
| 4 charged | $\pi^+\pi^-\pi^+\pi^-, K^+K^-\pi^+\pi^-, K_SK^\pm\pi^\mp$ |
| 4 charged + $\gamma$'s | $\pi^+\pi^-\pi^+\pi^-\pi^0, \pi^+\pi^-\eta, \pi^+\pi^-\omega, \pi^+\pi^-\pi^+\pi^-\pi^0\pi^0$, $K^+K^-\eta, K^+K^-\omega$ |
| 6 charged | $\pi^+\pi^-\pi^+\pi^-\pi^+\pi^-, K_SK^\pm\pi^\mp\pi^+\pi^-, K_SK_S\pi^+\pi^-$ |
| 6 charged + $\gamma$'s | $3(\pi^+\pi^-)\pi^0$ |
| Neutral | $\pi^0\gamma, \eta\gamma, \pi^0\pi^0\gamma, \pi^0\eta\gamma, \pi^0\pi^0\pi^0\gamma, \pi^0\pi^0\eta\gamma$ |
| Other | $n\bar{n}, \pi^0e^+e^-, \eta e^+e^-$ |
| Rare decays | $\eta'$, $D^*(2007)^0$ |

Work is in full swing.

# CMD-3 published results

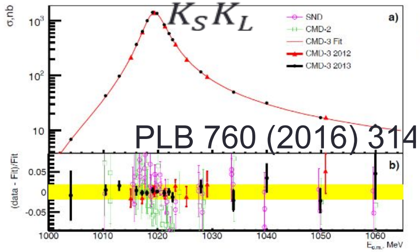


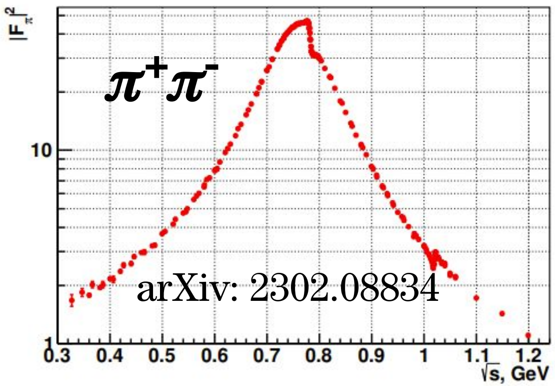


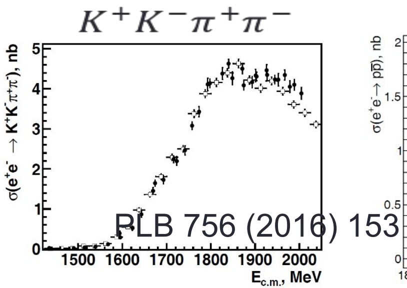


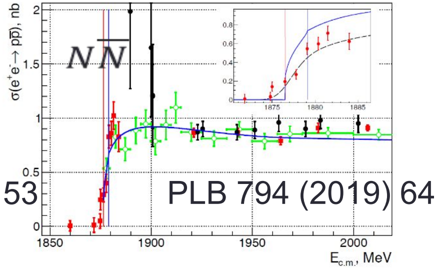


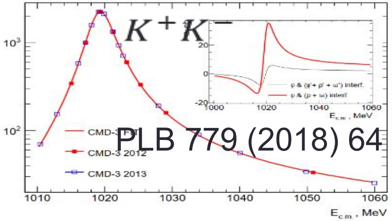


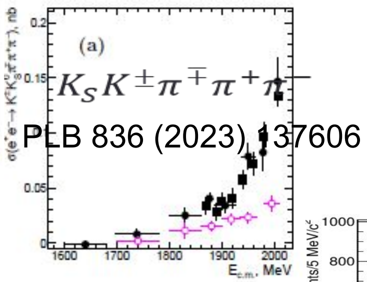


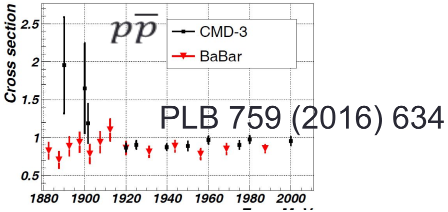


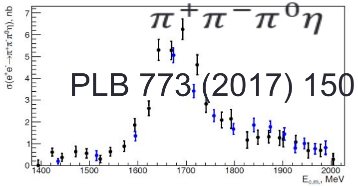


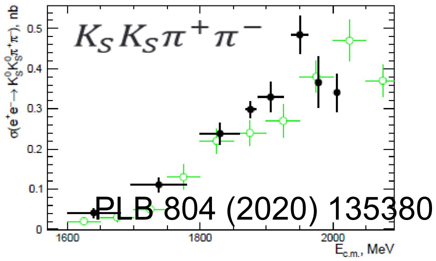


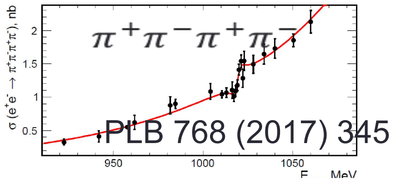


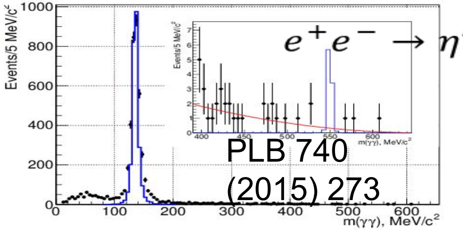


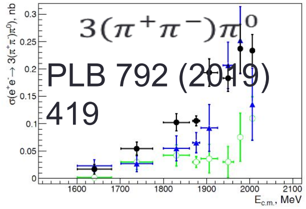


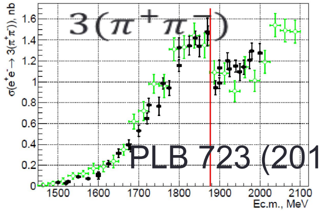


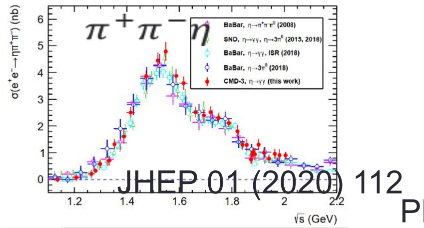


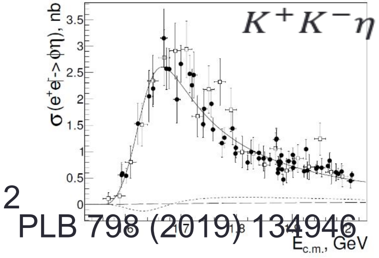

Let's focus on

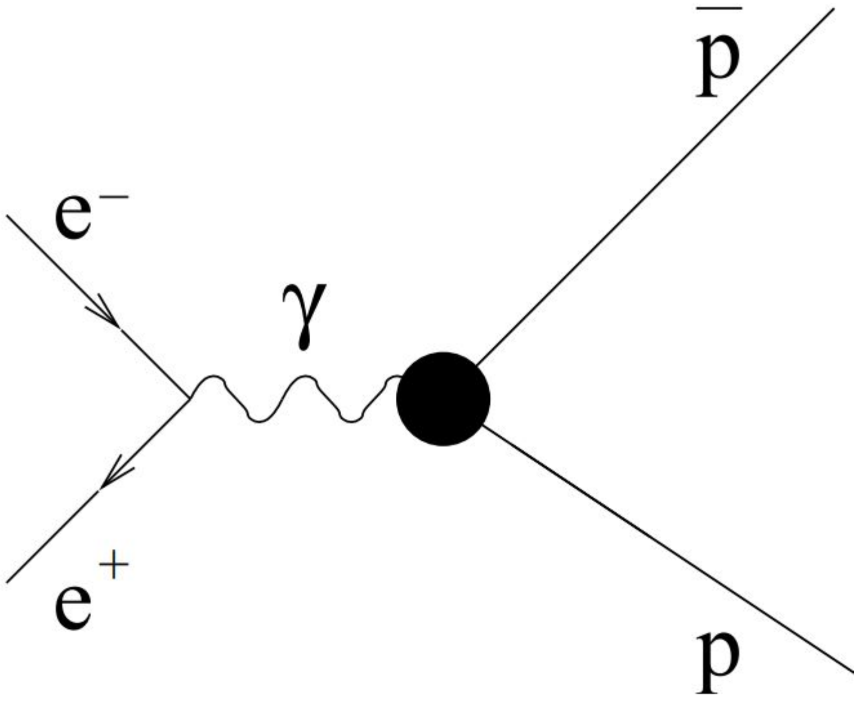

# Motivation

Phys. Lett. B 723 (2013) 73
Phys. Lett. B 794 (2019) 64–68

- NNbar cross section in the threshold energy region store information on (anti)nucleon internal structure (electro and magnetic FFs, i.e. $G_E$ and $G_M$).
- Due to the strong interaction in the final state xsection energy behaviour is complex.
- NNbar real reaction opening affects some of the multihadron cross sections in the form of a sharp dip.

However, there are still no precise experimental values of $G_E$ and $G_M$ in the threshold energy region.

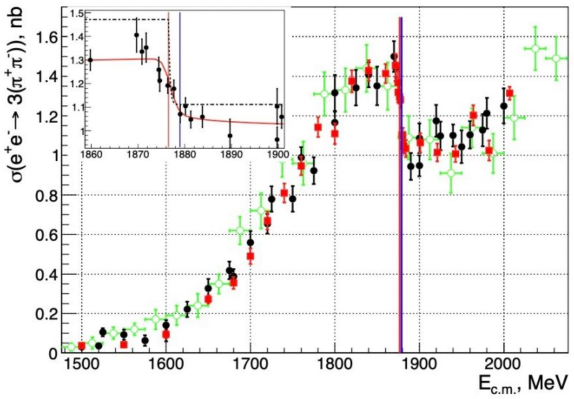


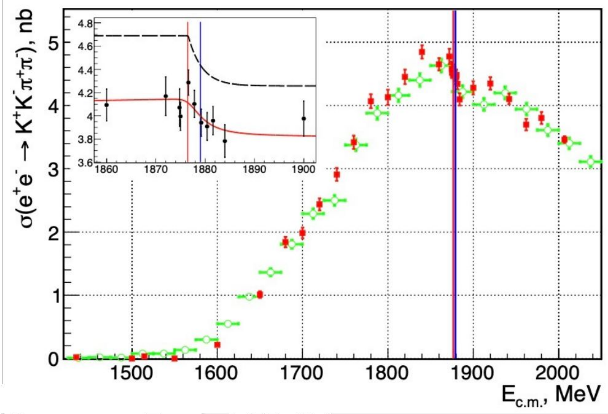


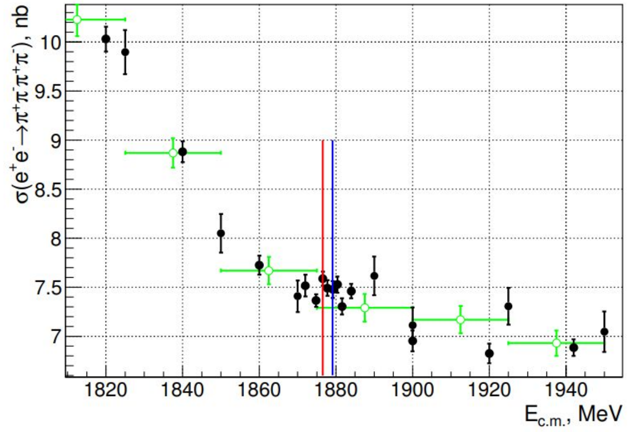

# Motivation

This process had been already studied at the CMD-3 (arXiv: 1507.08013 [hep-ex]). However, the amount of data drastically increased, and the workflow was improved.

The BaBar and BES III collaborations also studied the process in this energy region (doi:10.1103/PhysRevD.87.092005, arXiv:2102.10337). In these works, they used the ISR technique.

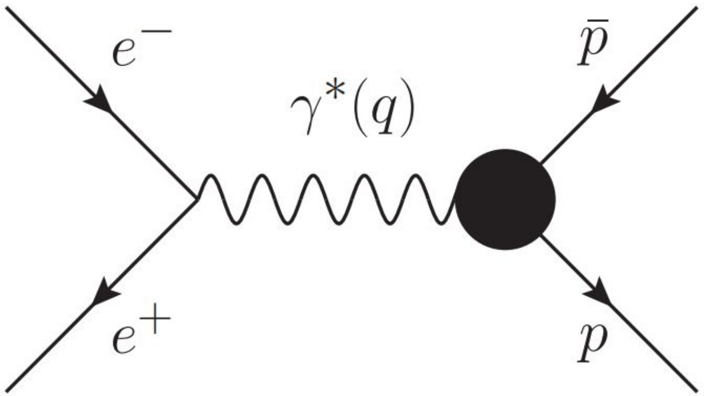


| Experiment | BaBar | BES III | CMD-3 (2017) | **This work** |
|---|---|---|---|---|
| Events | 2172 | 1386 | 2741 | **43416** |

| Season | **HIGH2017** | **HIGH2019** | **HIGH2020** | **HIGH2021** | **NNbar2022** | **Total** |
|---|---|---|---|---|---|---|
| ∫Ldt, $pb^{-1}$ | 22.68 | 16.44 | 37.34 | 47.83 | 128.74 | 253.05 |

# Event types

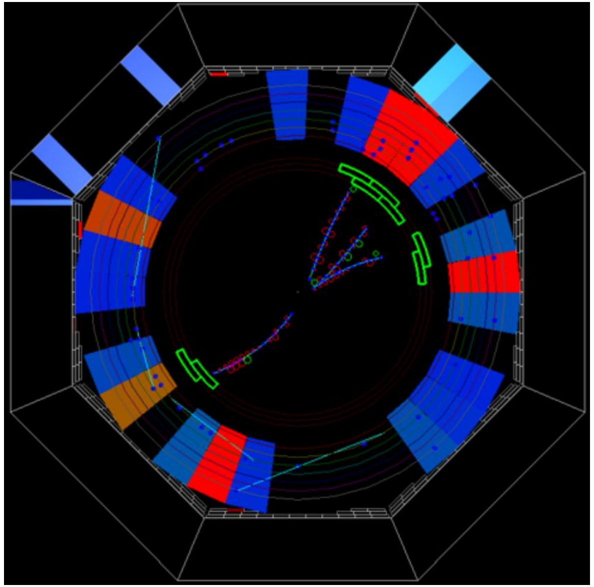

In the energy region close to the production threshold, antiprotons annihilate at the vacuum beam pipe or the DC inner wall (i.e. so-called annihilation star).

At higher energies, it is possible to detect the tracks of protons and antiprotons in the DC.

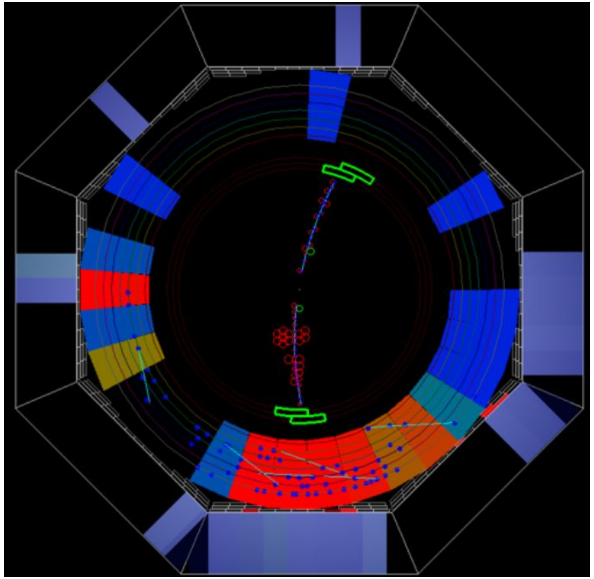

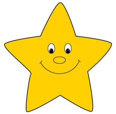

**“Stars”**

$E_{c.m.s} \lesssim 1.920$ GeV
$E_{beam} \lesssim 960$ MeV

Analysis workflows for these event types are **different**.

**Collinear events**

$E_{c.m.s} \gtrsim 1.920$ GeV
$E_{beam} \gtrsim 960$ MeV

# Collinear events

1. Event selection
2. Efficiency
3. $|G_E/G_M|$ measurement
4. Track reconstruction efficiency
5. Visible xsection

$E_{c.m.s} \gtrsim 1.920$ GeV
$E_{beam} \gtrsim 960$ MeV

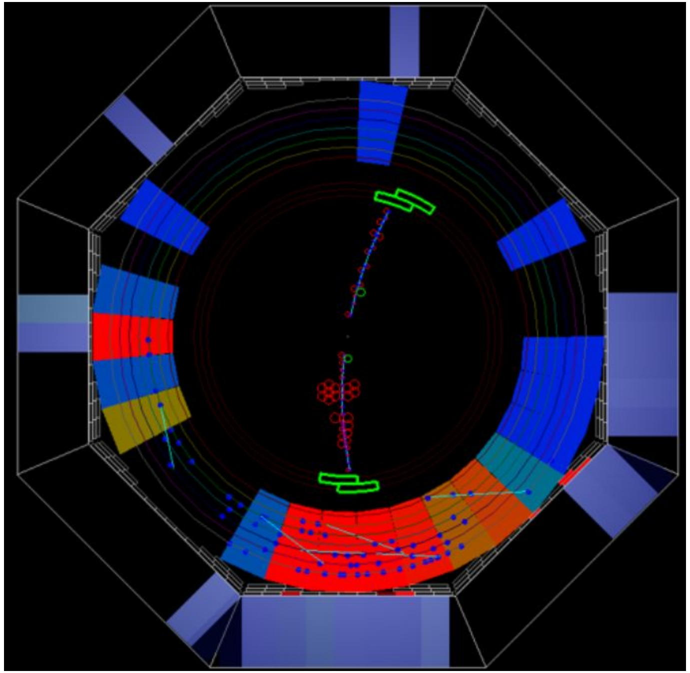

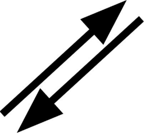

# Collinear Event selection

1. 2 tracks originating from the Interaction point: $\rho_{vertex} < 1$ cm and $|z_{track}| < 8$ cm
2. $\Delta\varphi = ||\varphi_{+} - \varphi_{-}| - \pi| < 0.15$ rad
3. $\Delta\theta = |\theta_{+} + \theta_{-} - \pi| < 0.2$ rad
4. Total energy deposition in calorimeters $E_{tot} > 200$ MeV
5. Tracks momenta correspond to proton/antiproton: $P < 1.3\sqrt{(E^2_{beam} - M^2_{proton})}$
6. Ionisation losses corresponds to protons.
7. Particles are in the fiducial volume: $|\cos(\theta)| < 0.7$

We counted all the events that passed the selection criteria.

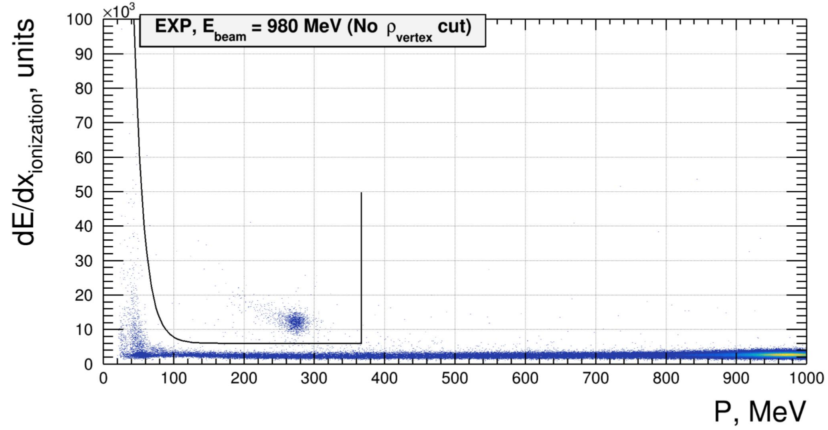


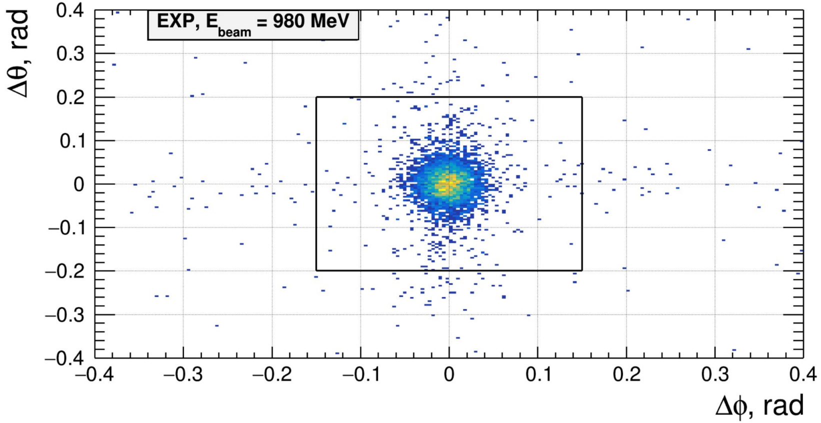

# Selection efficiency

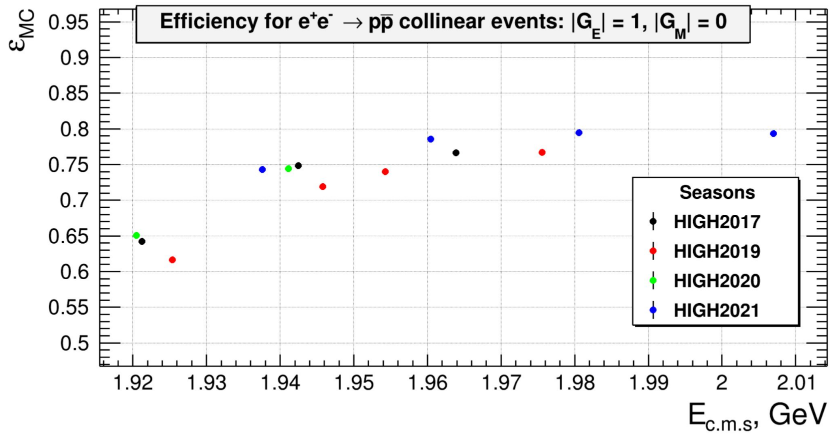


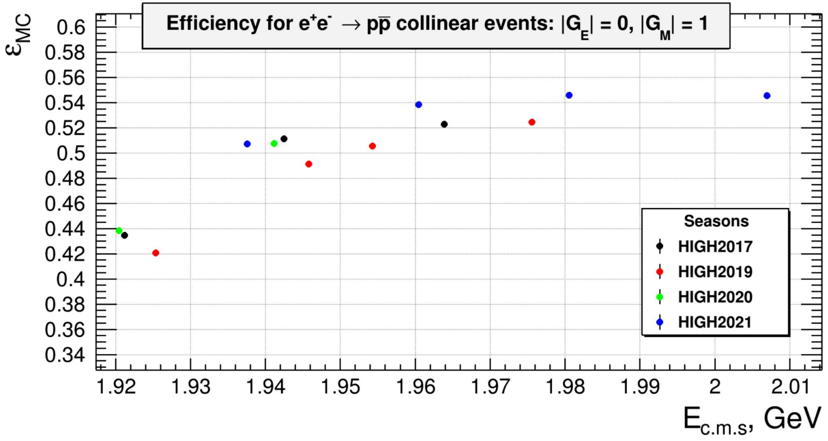


The cross section can be parameterized by two form factors, electrical $G_E$ and magnetic $G_M$, whose angular distributions are different.

$$\frac{dN}{dcos(\theta)} \propto \left[D_M(cos(\theta)) + \left|\frac{G_E(s)}{G_M(s)}\right|^2 D_E(cos(\theta))\right]$$

$D_{E,M}$ is an angular distribution of $G_{E,M}$ part.

$$D_E = sin^2(\theta_p)$$

$$D_M = 1 + cos^2(\theta_p)$$

The selection efficiency depends on the $|G_E/G_M|$.

# |$G_E/G_M$| measurement

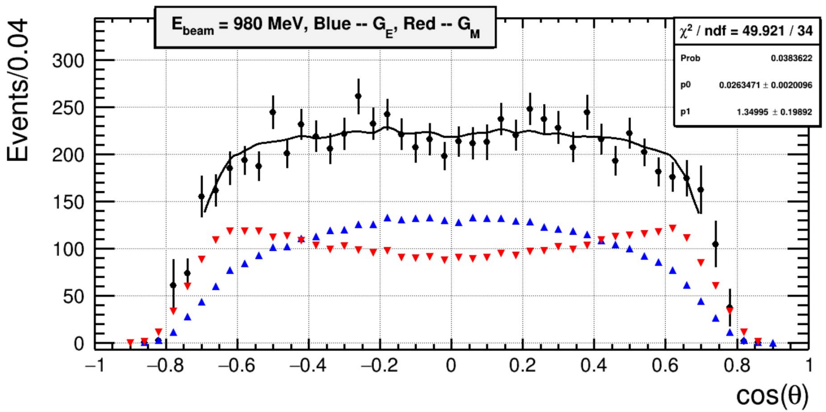


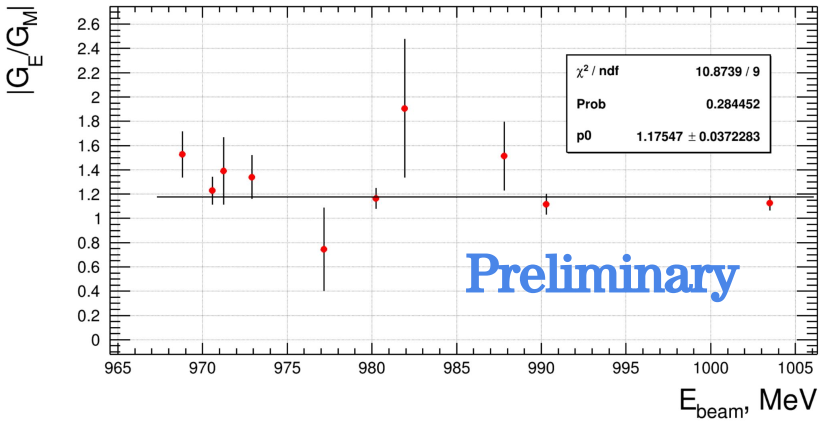


The cross section can be parameterized by two form factors, electrical $G_E$ and magnetic $G_M$, whose angular distributions are different.

The experimental data can be represented as the sum of two data samples: one with $|G_E| = 1$ and $|G_M| = 0$, and the second – vice versa.

Angular distribution of the experimental data was fitted with the following function:

$$\frac{dN}{dcos(\theta)} \propto \left[ D_M(cos(\theta)) + |\frac{G_E(s)}{G_M(s)}|^2 D_E(cos(\theta)) \right]$$

$D_{E,M}$ is an angular distribution of $G_{E,M}$.

The difference in track reconstruction efficiency in the MC and data was taken into account.

$$D^{(EXP)}_{\text{corrected}}(cos\theta) = D^{(EXP)}(cos\theta)\left(\frac{\varepsilon^{(MC)}_{track}}{\varepsilon^{(EXP)}_{track}}(cos\theta)\right)^2$$

# Track reconstruction efficiency

Antiproton selection criteria:

1) Track with $\rho_{track}$ < 0.2 cm and $|z_{tr}|$ < 4 cm
2) Negative charge
3) Ionisation losses and momentum correspond to antiprotons.

There are less than 3 tracks with $\rho_{track}$< 3 cm (multihadron event veto).

We paired found antiprotons with collinear protons:

1) Track with "good" $\chi^2$, $\rho_{track}$ < 0.2 cm, and $|z_{tr}|$ < 6 cm
2) Positive charge
3) Ionisation losses and momentum correspond to antiprotons.
4) $\Delta\varphi = ||\varphi_+ - \varphi_-| - \pi| < 0.15$ rad and $\Delta\theta = |\theta_+ + \theta_- - \pi| < 0.2$ rad

$$\varepsilon_{track} = \frac{N(p|\bar{p})}{N(\bar{p})}$$

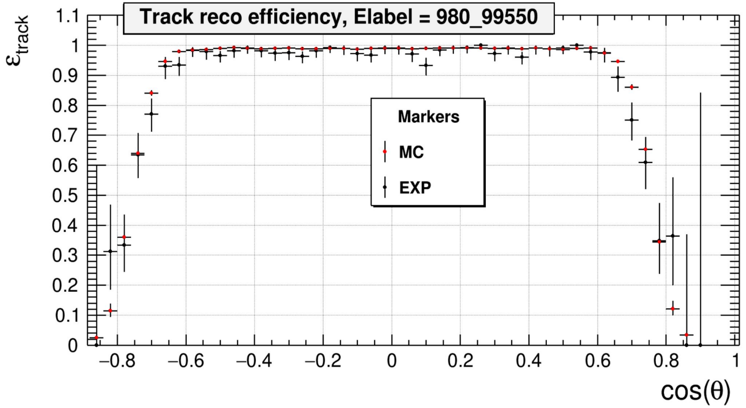


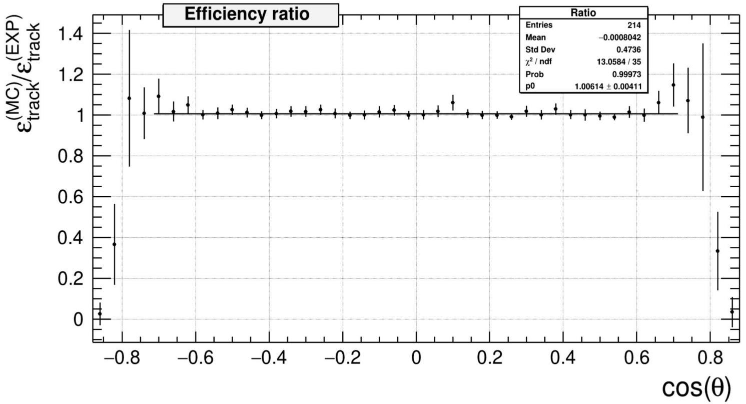

# Selection efficiency

MC sample with $|G_E/G_M| = 1.18 \pm 0.04$.

Efficiency statistical error arises from uncertainty of the $|G_E/G_M|$ ratio.

To take into account data-MC efficiency difference related to track reconstruction, we applied the correction:

$$\varepsilon_{EXP} = \varepsilon_{MC}\delta^{(+)}_{track}\delta^{(-)}_{track}, \quad \delta^{(+)}_{track} = \delta^{(-)}_{track} = \frac{\varepsilon^{(EXP)}_{track}}{\varepsilon^{(MC)}_{track}}$$

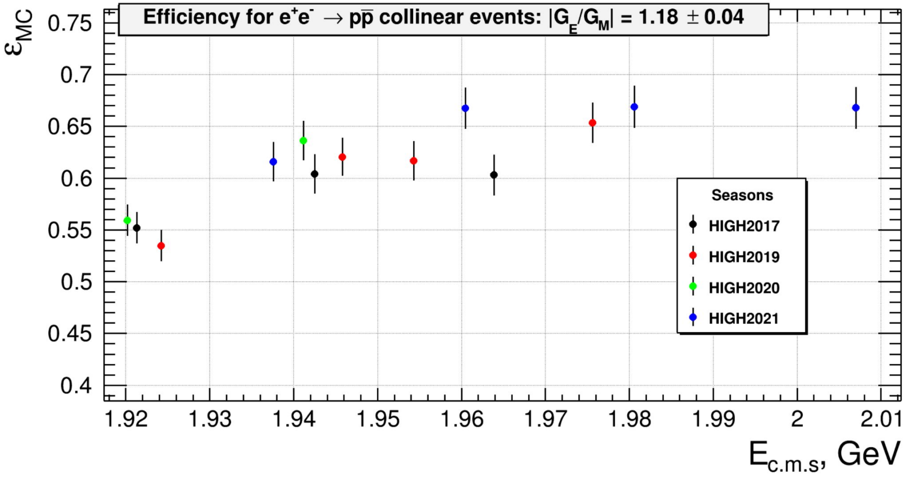


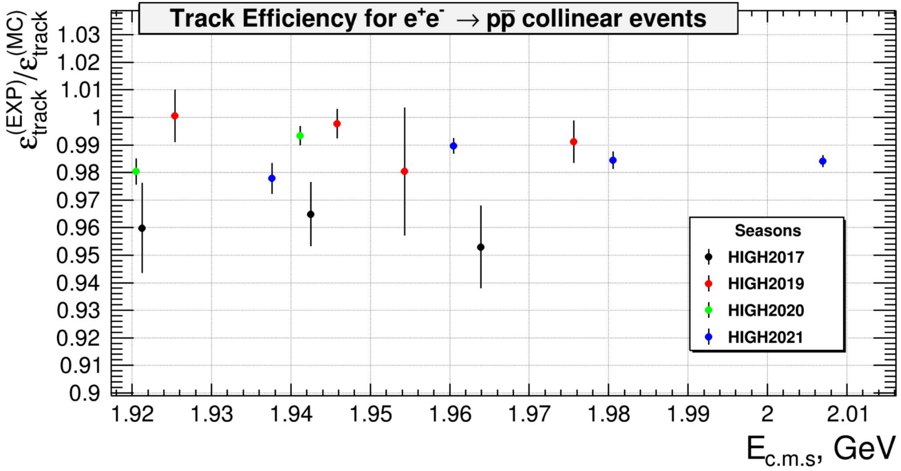

# Visible xsection

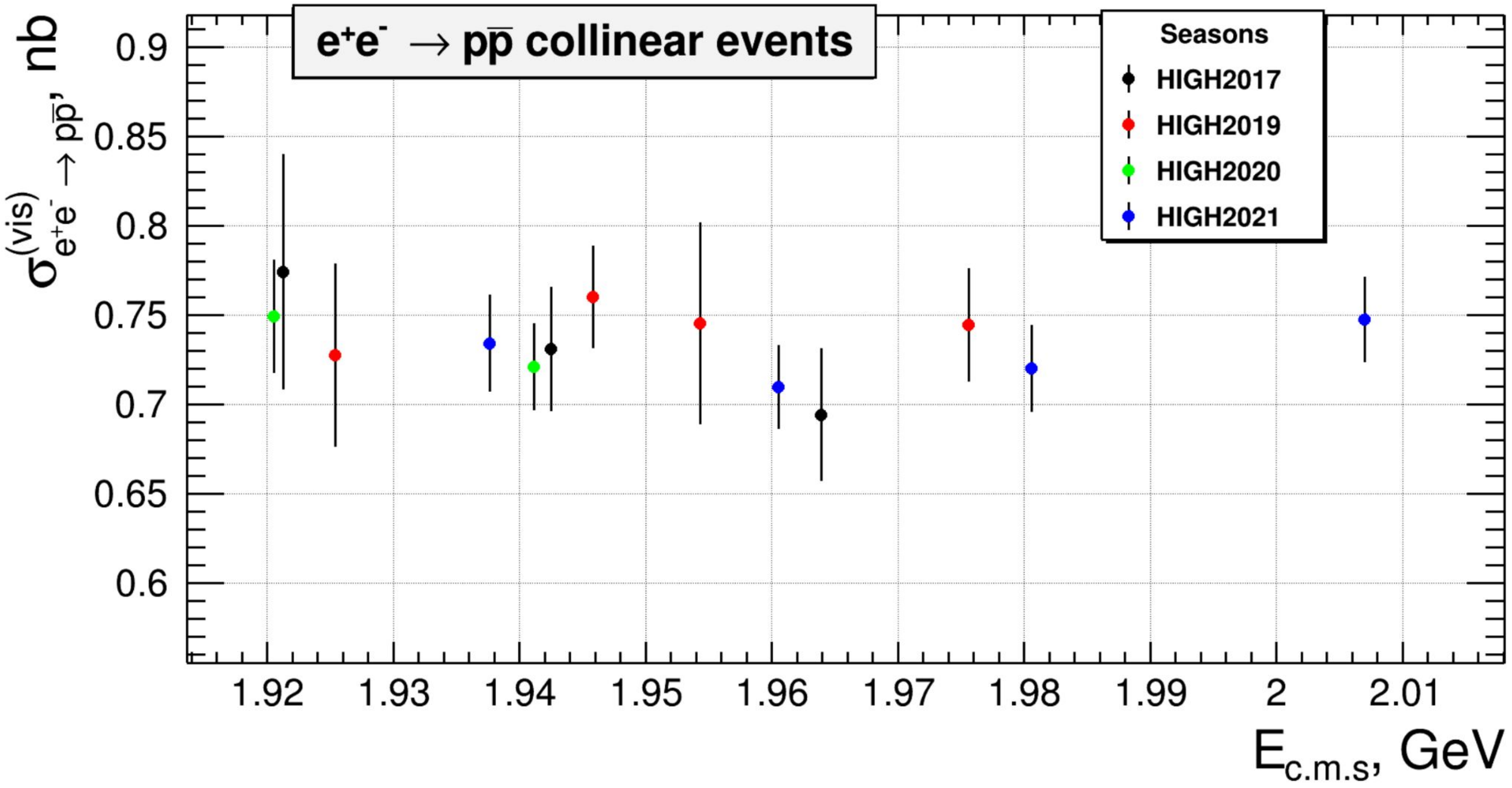

# “Stars”

1. Event selection
2. Event counting
3. Efficiency
4. Vacuum pipe thickness in the MC
5. Visible xsection

$E_{c.m.s} \lesssim 1.920$ GeV
$E_{beam} \lesssim 960$ MeV

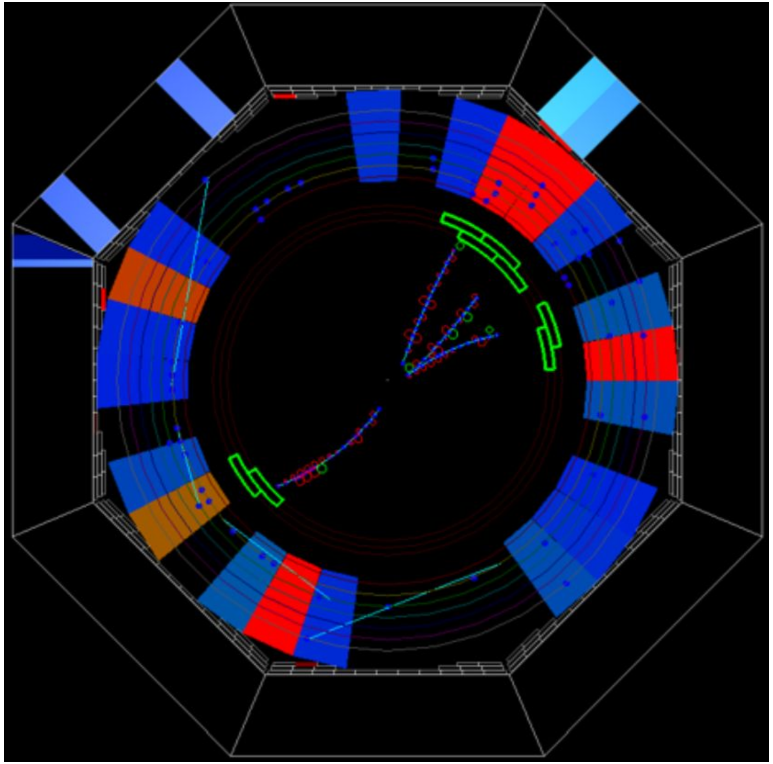

# Event selection

1. Track Energy deposition in calorimeters < 400 MeV,
2. There is a vertex that has at least 3 tracks with $\rho_{track}$ > 0.2 cm,
3. No secondary protons (from the vacuum pipe) in the vertex,
4. Total energy deposition in calorimeters $E_{tot}$ > 500 MeV
5. Minimal track momentum $p_{min}$ > 50 MeV
6. No collinear tracks in the vertex

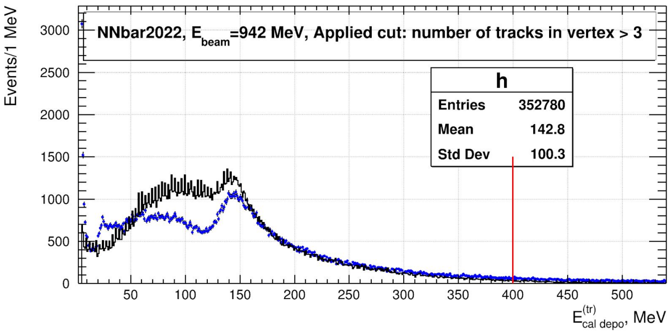


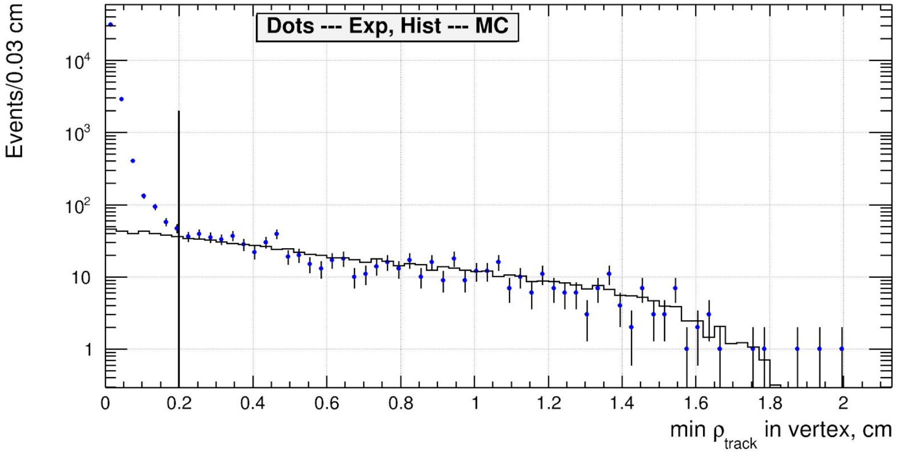


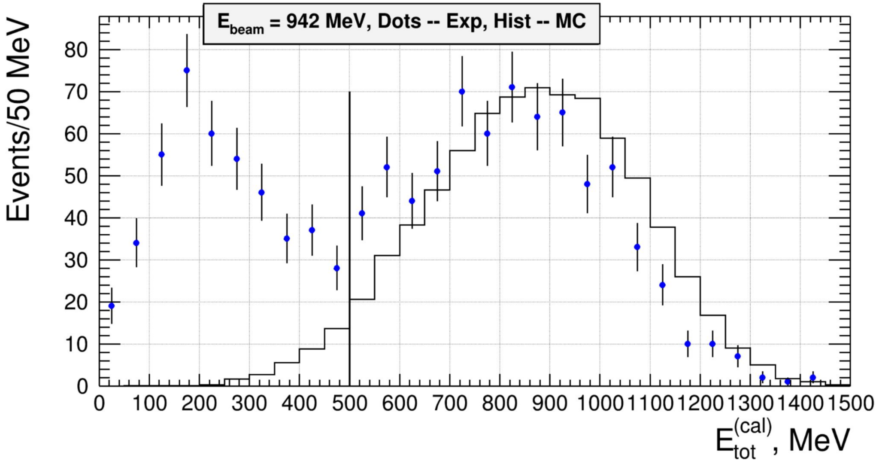

# Event counting

We obtained amount of the “stars” events in each energy point from the fit of $\rho_{vertex}$ distribution:
sig(MC) + bkg(expo + pol0) → data.
We used $|G_E/G_M| = 1.18 \pm 0.04$ to generate the MC sample.
The background model has ~2% systematic uncertainty

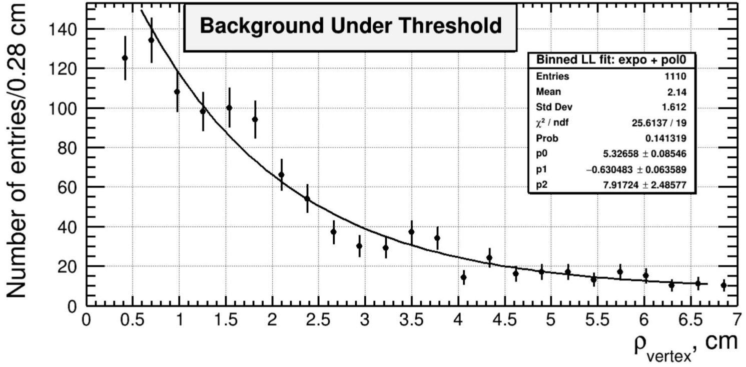


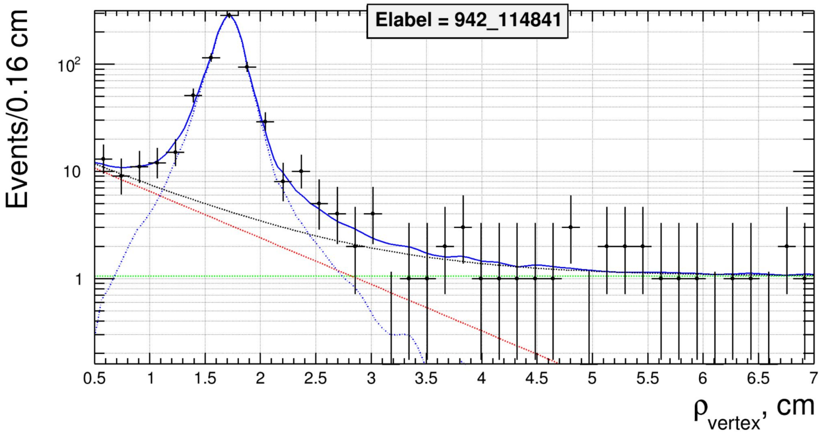


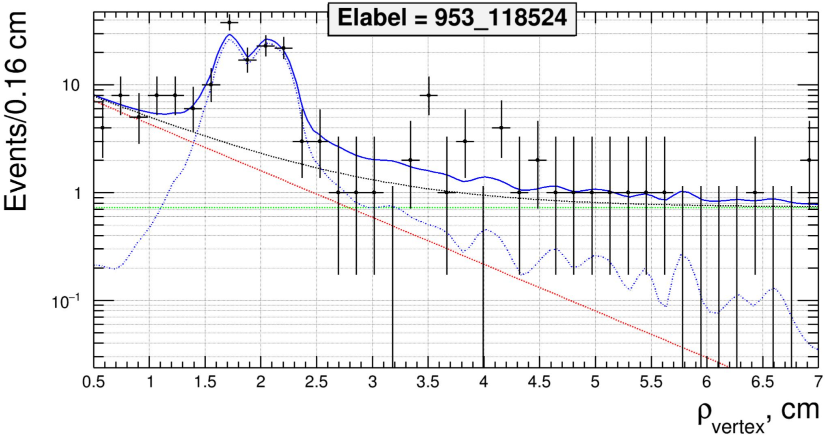

# Selection efficiency

$|G_E/G_M| = 1.18 \pm 0.04$

Antiprotons mainly annihilates at rest. But after 1.895 GeV antiprotons pass through the vacuum pipe => $\varepsilon_{MC}$ drops sharply at high energies.

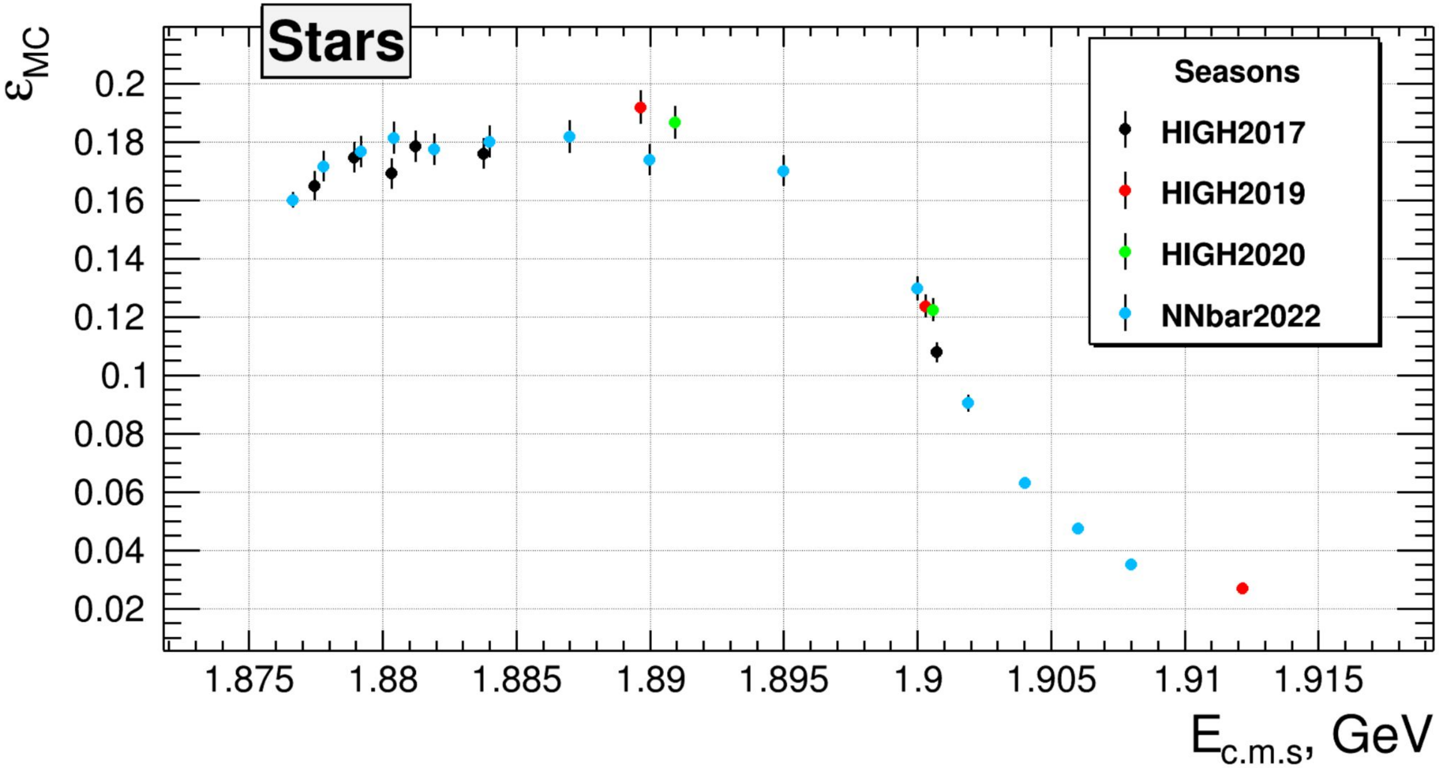

# Vacuum pipe thickness in MC

We suppose cross section to be constant in energy region 1.895 – 1.915 GeV. Due to MC simulation flaws (e.g. wrong dE/dx or material densities.) the $\varepsilon_{EXP} \neq \varepsilon_{MC}$.

We introduced the effective pipe thickness correction $\Delta_{pipe}$ to take into account these flaws.

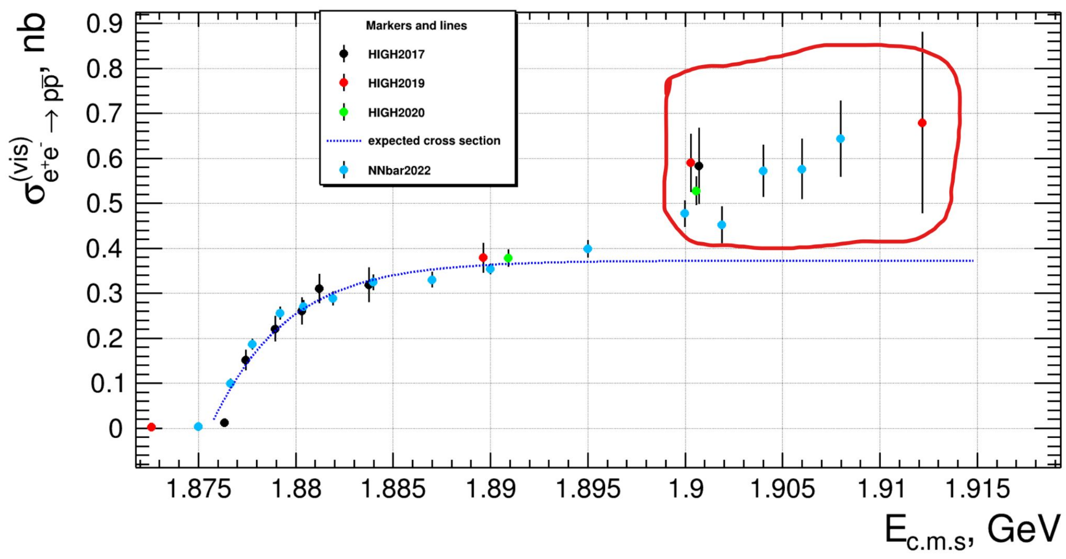


To obtain $\Delta_{pipe}$, we varied the pipe thickness in the MC.

$$\frac{\sigma_{found}}{\sigma_{expected}} = \frac{\varepsilon_{MC}^{(standard)}}{\varepsilon_{MC}^{(varied)}}$$

# Vacuum pipe thickness in MC

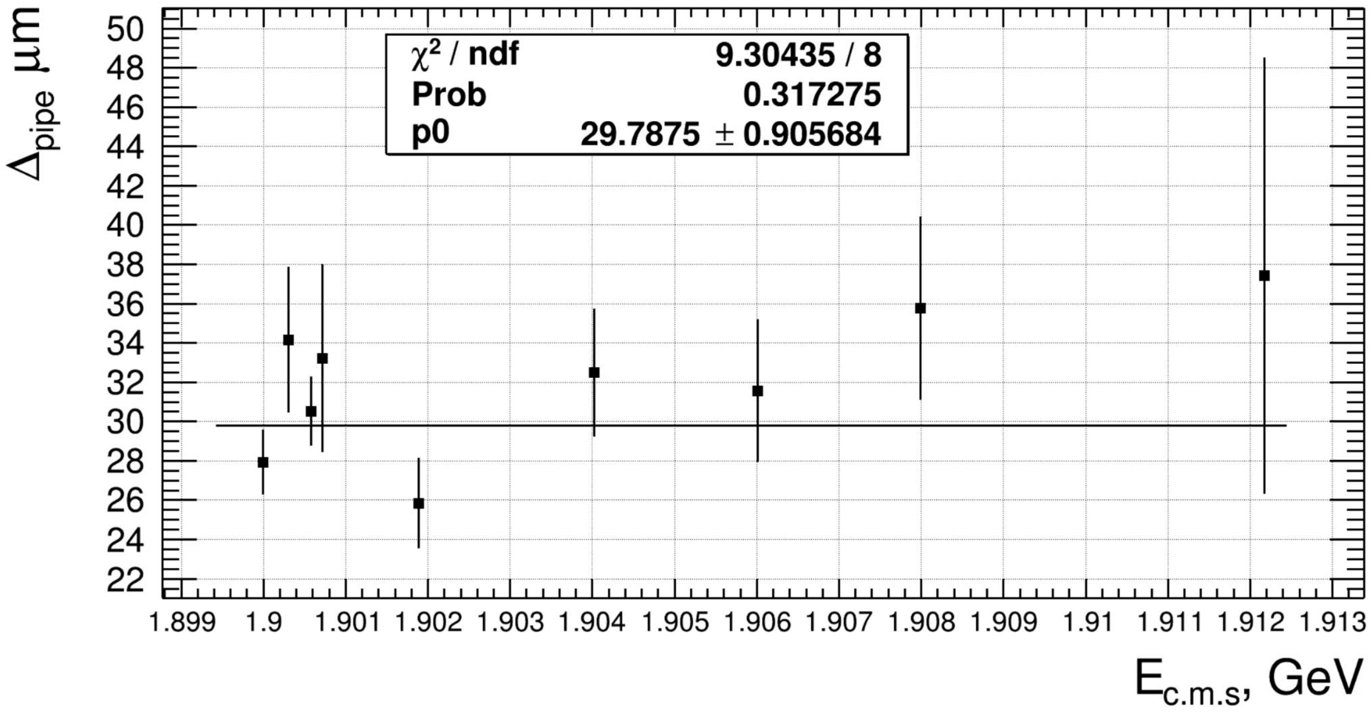


$$\Delta_{\text{pipe}} \approx (5.81 \pm 0.26)\% = (29.79 \pm 0.9)\ \mu m$$

# Visible xsection

GENAT4 correctly simulates energy dependence of the antiproton probability to stop in the material. But the annihilation at rest doesn't. Hence, we don't know energy-independent factor of the selection efficiency **P(annihilation)**.

$$\varepsilon_{MC} = P(stop)P(annihilation)\varepsilon(selection|annihilation)$$

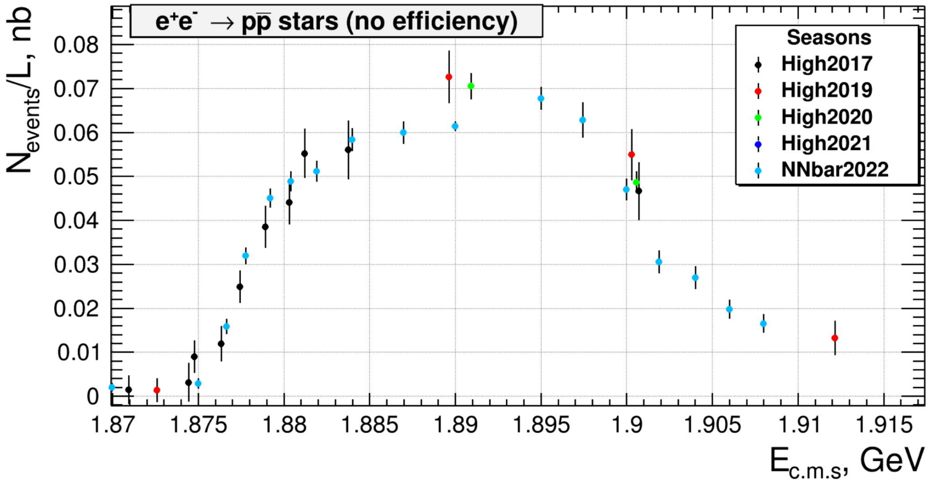


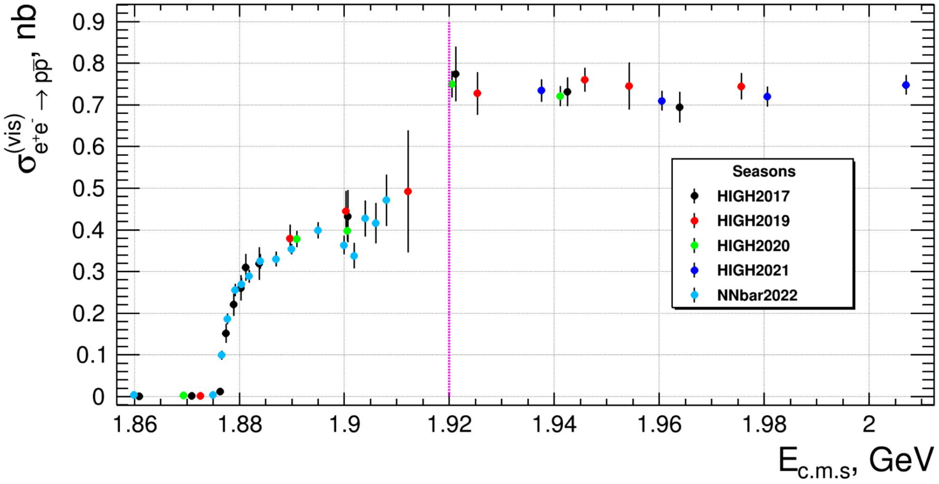

# The visible cross section fit

$$\sigma_{born} = \theta(E_{c.m.s.} - threshold) * level * (1 - e^{-slope*(E_{c.m.s.} - threshold)})$$

$$* \; \sigma_{vis}(s) = \frac{1}{\sqrt{2\pi\sigma_E^2(s)}} \int_{\infty}^{\infty} e^{-\frac{(E_{c.m.s} - \sqrt(s))^2}{2\sigma_E^2(s)}} \times$$

$$\int_0^{1 - s_T/E^2_{c.m.s}} F(x, E^2_{c.m.s})\sigma_{born}(E^2(1-x))dxdE$$

$$\chi^2 = (\sigma^{(eval)} - \sigma^{(data)}/k_{stars})/\Delta\sigma^{*2}$$

$$k_{stars} = \begin{cases} \text{free parameter, if } E_{beam} < 955 \text{ MeV}, \\ 1 \text{ if } E_{beam} > 955 \text{ MeV, fixed} \end{cases}$$

$k_{stars}$ — efficiency correction due to P\bar{P} annihilation cross-section value in the Geant4

$\chi^2/ndf = 24/39$

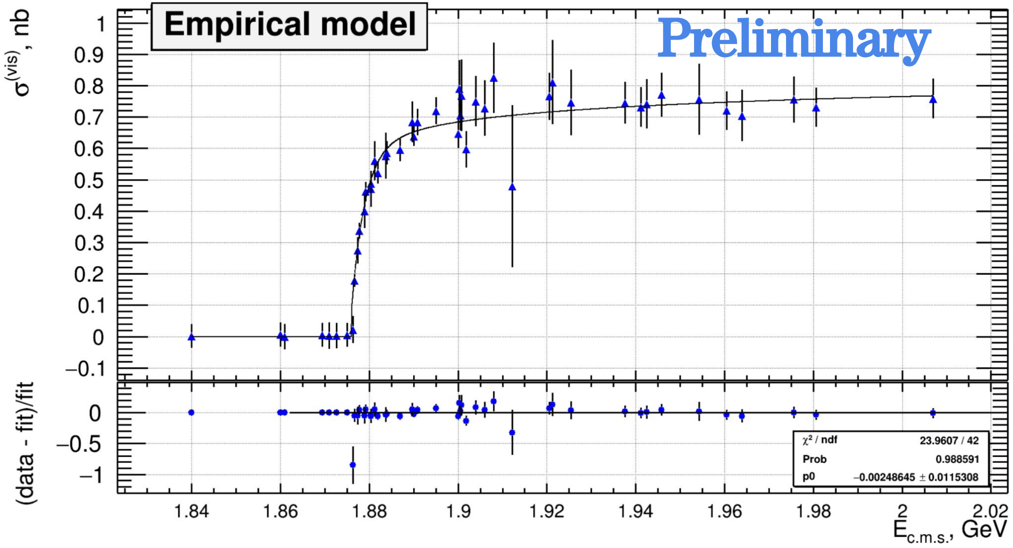


| Pos | Name | type | Value | Error +/- |
|---|---|---|---|---|
| 0 | threshold | free | 1.8755 | 0.0003 |
| 1 | level | free | 0.850 | 0.011 |
| 2 | slope | free | 382.5 | 71.3 |
| 3 | k_stars | free | 0.5544 | 0.0147 |

* arXiv: 2108.07539 [hep-ex]

# Results

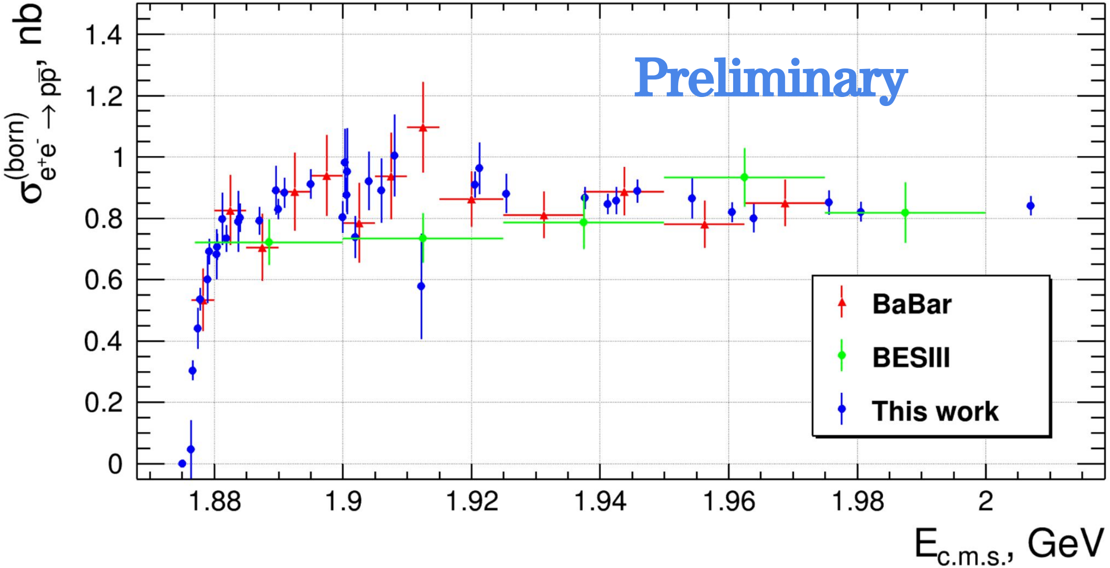


Table 3: Systematic uncertainties for the collinear events.

| Source | Average value | Maximum Value |
|---|---|---|
| Collinearity cut | 0.3% | 0.7% |
| Other selection criteria | 0.25% | 0.3% |
| $\|G_E/G_M\|$ | 2% | 3% |
| Luminosity | 1% | 1% |
| Radiative correction | 1% | 1% |
| Track reconstruction | 1.5% | 3% |
| Total | 2.9% | 4.5% |

Table 2: Systematic uncertainties for the "Stars" events.

| Source | Average value | Maximum Value |
|---|---|---|
| Total energy deposition cut | 4.7% | 9% |
| $\rho_{vertex}$ cut | 0.5% | 0.8% |
| Event counting | 2% | 2% |
| Luminosity | 1% | 1% |
| Radiative correction | 1% | 1% |
| $\|G_E/G_M\|$ | 1.5% | 1.5% |
| Tube width uncertainty | 2% | 2% |
| $k_{stars}$ value | 5% | 5% |
| Total | 7.7% | 10.9% |

This work (**Preliminary**): $|G_E/G_M| = 1.18 \pm 0.04 \pm 0.06$ if $1.92\ \text{GeV} < E_{c.m.s} < 2.007\ \text{GeV}$

$$\text{BESIII (ISR)}: |G_E/G_M| = \begin{cases} 1.27 \pm 0.23 \pm 0.09, & \text{if } 1.877\ \text{GeV} < M_{p\bar{p}} < 1.950\ \text{GeV}, \\ 1.78 \pm 0.33 \pm 0.11, & \text{if } 1.950\ \text{GeV} < M_{p\bar{p}} < 2.025\ \text{GeV} \end{cases}$$

arXiv:2102.10337 [hep-ex]

BESIII (2020): $|G_E/G_M| = 1.38 \pm 0.10 \pm 0.03$ ($E_{c.m.s} = 2.0$ GeV)

arXiv:2102.10337 [hep-ex]

$$\text{BaBar(ISR)}: |G_E/G_M| = \begin{cases} 1.36^{+0.15+0.05}_{-0.14-0.04}, & \text{if } 1.877\ \text{GeV} < M_{p\bar{p}} < 1.950\ \text{GeV} \\ 1.48^{+0.16+0.06}_{-0.14-0.05}, & \text{if } 1.950\ \text{GeV} < M_{p\bar{p}} < 2.025\ \text{GeV} \end{cases}$$

doi:10.1103/PhysRevD.87.092005

# Back up

# Born cross section parametrization

$$\sigma_{p\bar{p}}(s) = \frac{4\pi\alpha\beta C}{3s}\left[|G_M(s)|^2 + \frac{2M_p^2}{s}|G_E(s)|^2\right]$$

$$C = y/(1-e^{-y}),\ y = \pi\alpha/\beta,\ \beta = \sqrt{1-4M_p^2/s}$$

# Pipe thickness correction

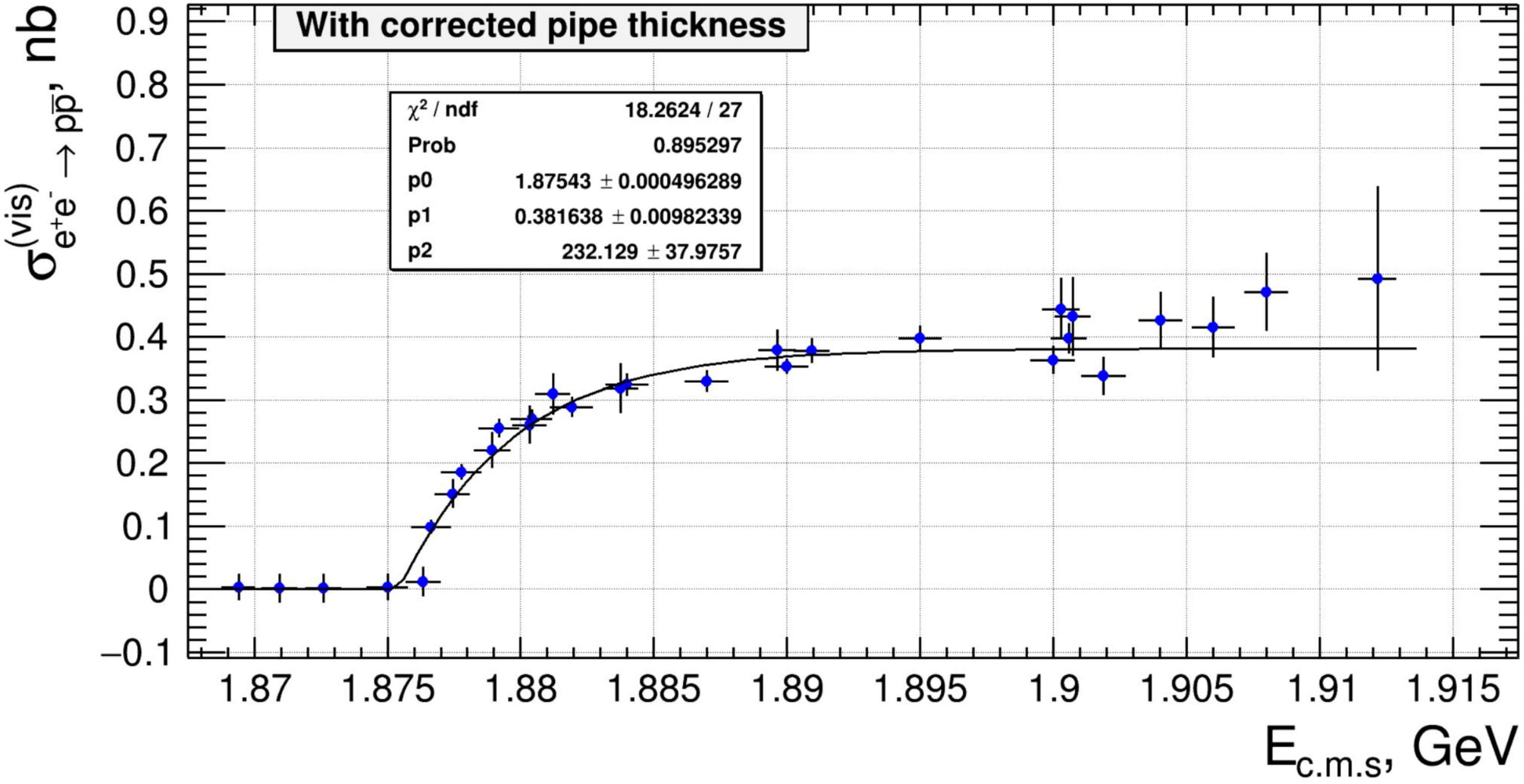

# Pipe thickness correction

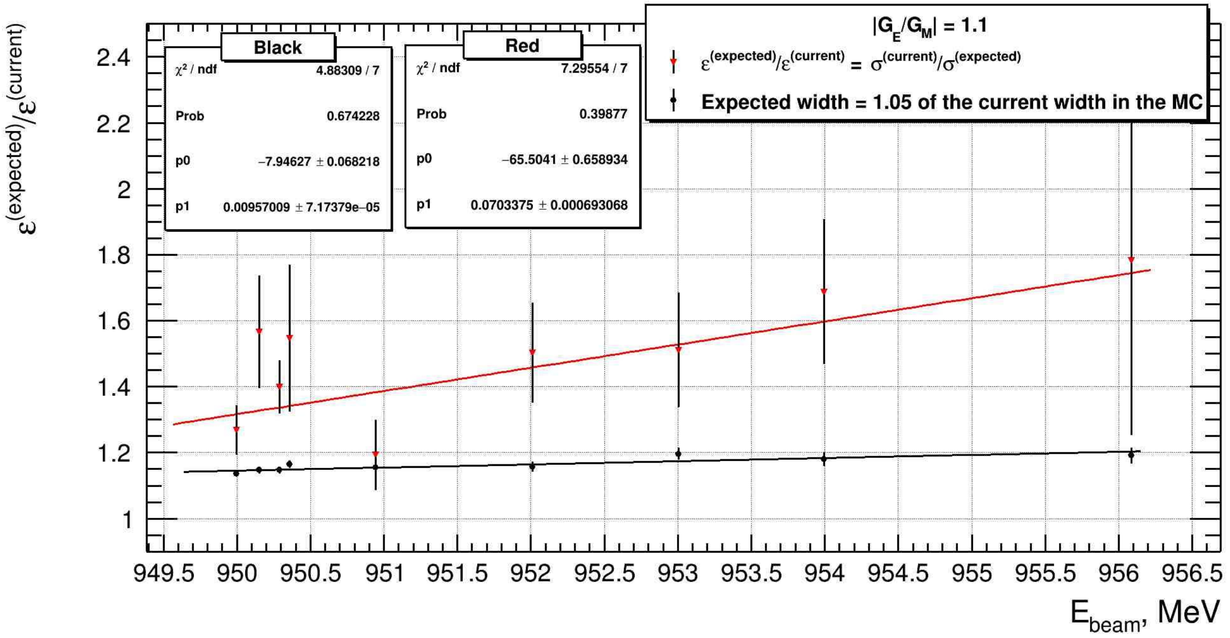

# Comparison with the phenomenology

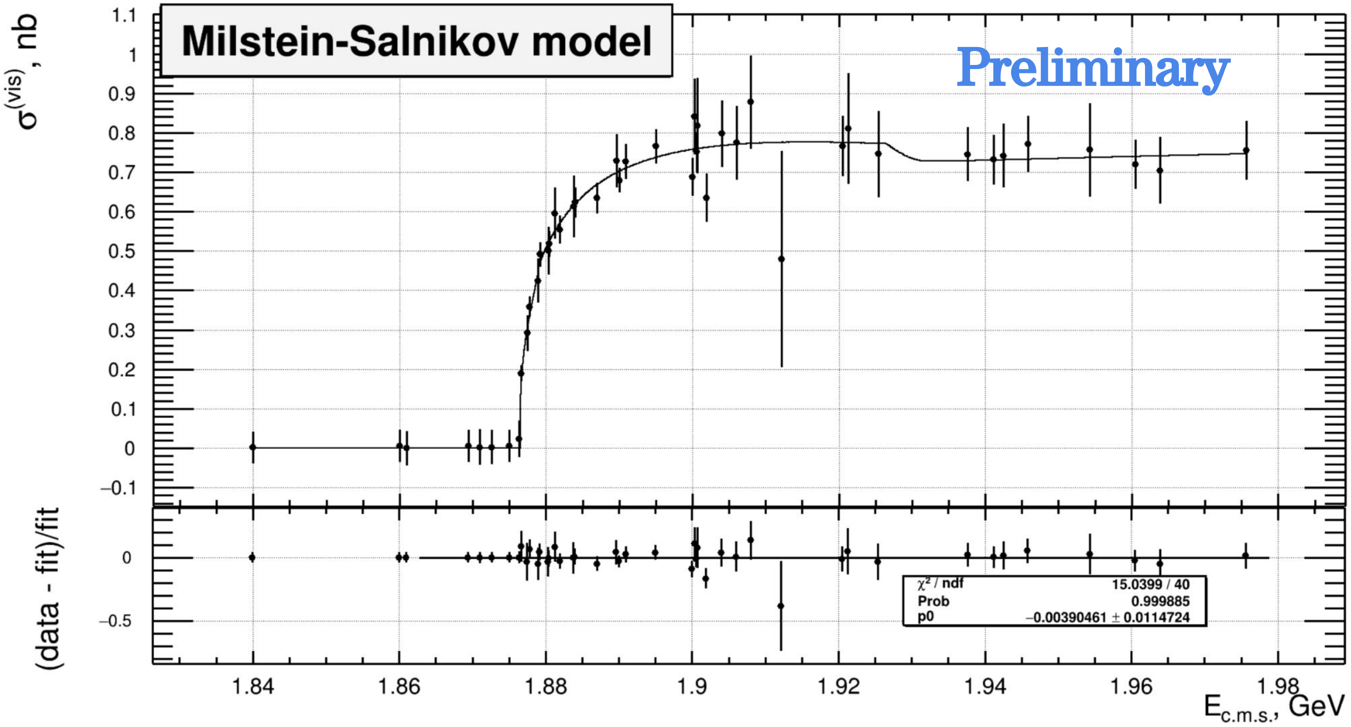


$\chi^2$/ndf = 15/41

| Name | type | Value | Error +/- |
|---|---|---|---|
| threshold | fixed | 1.87654 GeV | 0.001 GeV |
| scale | free | 1.029 | 0.015 |
| k_stars | free | 0.5211 | 0.0115 |

arXiv: 2207.14020 [hep-ph]